AGU PUBLICATIONS

JGR

Journal of Geophysical Research: Atmospheres

RESEARCH ARTICLE

10.1002/2013JD020555

Key Points:

- Surface ozone variability at Highveld is examined during 1990–2007
- ENSO and NOx affects surface ozone over the South African Highveld
- Surface ozone on the Highveld has not increased over 1990–2007

Correspondence to:
N. V. Balashov,
nvb5011@psu.edu

Citation:
Balashov, N. V., A. M. Thompson, S. J. Piketh, and K. E. Langerman (2014), Surface ozone variability and trends over the South African Highveld from 1990 to 2007, *J. Geophys. Res. Atmos.*, *119*, doi:10.1002/2013JD020555.

Received 12 JUL 2013
Accepted 27 FEB 2014
Accepted article online 3 MAR 2014

Surface ozone variability and trends over the South African Highveld from 1990 to 2007

Nikolay V. Balashov[1], Anne M. Thompson[1,2,3], Stuart J. Piketh[4], and Kristy E. Langerman[5]

[1]Department of Meteorology, Pennsylvania State University, University Park, Pennsylvania, USA, [2]Now at NASA/Goddard Space Flight Center, Greenbelt, Maryland, USA, [3]School of Natural Sciences, North-West University, Potchefstroom, South Africa, [4]School of Geo and Spatial Science and Unit for Environmental Science and Management, North-West University, Potchefstroom, South Africa, [5]Environmental Management Department, Eskom, Johannesburg, South Africa

Abstract Surface ozone is a secondary air pollutant formed from reactions between nitrogen oxides ($NO_x = NO + NO_2$) and volatile organic compounds in the presence of sunlight. In this work we examine effects of the climate pattern known as the El Niño–Southern Oscillation (ENSO) and NO_x variability on surface ozone from 1990 to 2007 over the South African Highveld, a heavily populated region in South Africa with numerous industrial facilities. Over summer and autumn (December–May) on the Highveld, El Niño, as signified by positive sea surface temperature (SST) anomalies over the central Pacific Ocean, is typically associated with drier and warmer than normal conditions favoring ozone formation. Conversely, La Niña, or negative SST anomalies over the central Pacific Ocean, is typically associated with cloudier and above normal rainfall conditions, hindering ozone production. We use a generalized regression model to identify any linear dependence that the Highveld ozone, measured at five air quality monitoring stations, may have on ENSO and NO_x. Our results indicate that four out of the five stations exhibit a statistically significant sensitivity to ENSO at some point over the December–May period where El Niño amplifies ozone formation and La Niña reduces ozone formation. Three out of the five stations reveal statistically significant sensitivity to NO_x variability, primarily in winter and spring. Accounting for ENSO and NO_x effects throughout the study period of 18 years, two stations exhibit statistically significant negative ozone trends in spring, one station displays a statistically significant positive trend in August, and two stations show no statistically significant change in surface ozone.

1. Introduction

The South African provinces of Mpumalanga, Gauteng, and Free State partially comprise a region known as the Highveld (Figure 1)—a plateau with elevations ranging from approximately 1 to 2 km. The region is home to the most industrialized and populous section of the country, containing the majority of South African coal-fired power plants along with about 27% of households [*Statistics South Africa*, 2012; *Tyson et al.*, 1988]. Air pollution has long been recognized as a significant issue for the Highveld, but extensive documentation of this topic is not widely available in the peer-reviewed literature [*Laakso et al.*, 2008]. For instance, because many households cannot afford to use electricity for cooking and especially heating, serious issues regarding indoor air pollution, resulting from burning of coal and kerosene among other fuels, ensue [*Liousse et al.*, 2012; *Norman et al.*, 2007]. In the atmosphere criteria, pollutants such as nitrogen oxides ($NO_x = NO + NO_2$), ozone (O_3), carbon monoxide (CO), particulate matter, and sulfur dioxide (SO_2) exceed World Health Organization levels over the industrialized Highveld, contributing to a high rate of acute respiratory infections [*Liousse et al.*, 2012; *Matooane et al.*, 2004]. In this paper we focus explicitly on surface ozone over the Highveld area for the approximate time period of 1990–2007.

Surface ozone is a secondary air pollutant formed from reactions between NO_x and volatile organic compounds (VOCs) in the presence of sunlight. [*Jenkin and Clemitshaw*, 2000]. It is generally agreed that relatively high concentrations of ozone have negative effects on human lung functions [*Uysal and Schapira*, 2003] and crop production [*Avnery et al.*, 2011]. One focus of the Southern African Fire-Atmosphere Research Initiative in 1992 (SAFARI-92) was to understand how biomass burning affects ozone over southern Africa by emitting essential gaseous precursors [*Fishman et al.*, 1996; *Thompson et al.*, 1996]. The campaign mainly concentrated on tropospheric ozone; however, this led to important findings regarding the regional ozone seasonal cycle. Typically, tropospheric ozone over the Highveld reaches its peak during the southern hemispheric spring

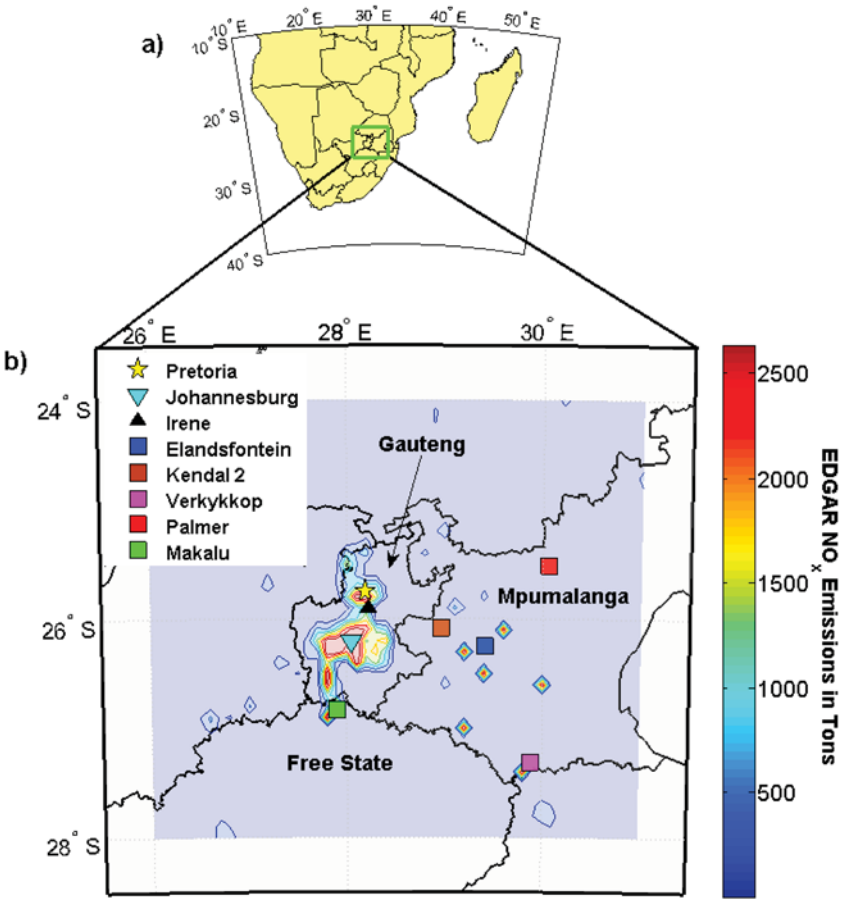

Figure 1. (a) Map of southern Africa. (b) Map of northeastern South Africa indicating provinces that approximately comprise the Highveld industrial center, long-term air quality monitoring stations, Irene weather station, and the location of Johannesburg-Pretoria nexus. The map is overlaid with the median of yearly EDGAR NO_x emissions during 1990–2007 time period. Source: EC-JRC/PBL. EDGAR version 4.2. http://edgar.jrc.ec.europa.eu/, 2011.

months of September–October–November (SON) and minimum values are in the autumn months of March–April–May (MAM) [*Diab et al*., 1996]. The ozone maximum in SON originates from a variety of sources, including seasonal biomass burning, a process that includes savanna fires, forest fires, agricultural waste combustion, and domestic biofuel combustion. A semipermanent anticyclonic pattern with vertical stable layers allows pollutants to accumulate in these layers; stratospheric intrusions caused by westerly waves also add to the tropospheric ozone burden [*Diab et al*., 2004]. Burning processes result in the emission of CO, methane (CH_4), NO_x, and nonmethane hydrocarbons that are the precursors to photochemical O_3 formation [*Marufu et al*., 2000]. The ozone minimum often occurs in MAM, although this is more complicated because different layers of the troposphere may reach seasonal minimum values at various times from summer (December–January–February, DJF) through autumn (MAM) depending on a number of complex meteorological conditions that vary from year to year [*Diab et al*., 2003, 2004].

Stevens [1987] counted 84 cases from September 1984 to August 1985 in which the Johannesburg area exceeded an 80 ppbv surface ozone hourly average. *Combrink et al*. [1995] analyzed surface ozone data from two sites on the Highveld: Elandsfontein in the middle of the industrialized area and Verkykkop that is generally downwind of the industrialized area. They found that on average at both locations, ozone typically peaks between 1400 and 1700 h (local time) due to photochemical formation, which is typical of a polluted environment. *Combrink et al*. [1995] also analyzed monthly surface ozone cycles from 1988 to 1991 and reported maxima in SON and minima in DJF. *Rorich and Galpin* [1998] calculated trends of several trace gases at four monitoring stations located in and downwind of the industrialized areas on the Highveld—Elandsfontein, Verkykkop, Palmer, and Makalu—from 1984 to 1994 and found no significant trends in ozone concentrations

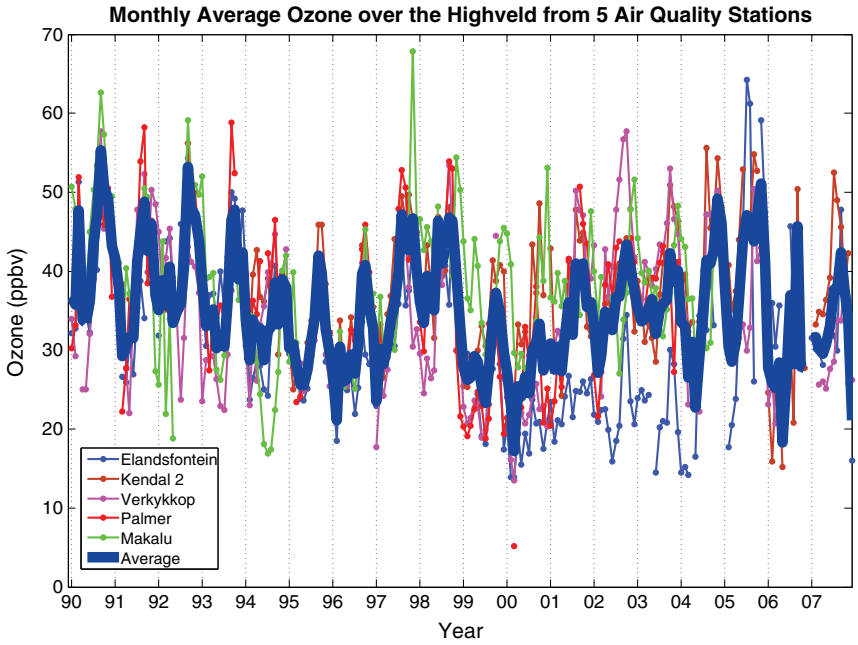

Figure 2. Eighteen years (1990–2007) of monthly ozone averages (calculated from diurnal 1100–1600 local time averages) over the Highveld from Elandsfontein (blue), Kendal 2 (brown), Verkykkop (magenta), Palmer (red), and Makalu (green). Dark blue indicates average of all the stations.

at all of the sites except Verkykkop. *Clain et al*. [2009] used ozonesondes from the Irene site, located near Pretoria, to calculate ozone trends for different layers over the 1990–2007 time period. The study found a statistically significant positive surface ozone trend for Irene; however, the data set used was missing 1994–1997 data and suffered from inconsistent launch times [*Balashov et al*., 2013; A. Thompson et al., Is tropospheric ozone over Southern Africa really increasing? Evidence from sonde and aircraft profiles submitted to *Atmospheric Chemistry and Physics*, 2014]. A few other studies have addressed spatial ozone variability in southern Africa [*Josipovic et al*., 2010; *Laakso et al*., 2012; *Lourens et al*., 2011; *Zunckel et al*., 2004], but these have not examined ozone oscillations over extended periods of time at the Highveld.

Year-to-year ozone fluctuations over the Highveld are substantial (Figure 2). In many cases, NO_x may be considered as the limiting ozone precursor and therefore an important predictor of ozone variability [*Sillman*, 1999]. Figure 3 shows time series and monthly anomalies of NO_x corresponding to the ozone time series in Figure 2. The variability of NO_x is complicated at the Highveld because different stations are affected by different sources (see Figure 1). No clear trend of NO_x mixing ratios from the stations (Figure 3b) is apparent in the region despite the fact that the Highveld NO_x emissions have probably increased about 20% over the 1990–2007 interval (Source: EC-JRC/PBL. EDGAR version 4.2. http://edgar.jrc.ec.europa.eu/, 2011). One possible reason for this discrepancy is that monitoring stations do not correspond to locations with the most emissions (Figure 1). It is important to note that in general ozone is not proportional to NO_x over the Highveld; in-depth discussion of this topic can be found in section 2.1 (see Figure 6 and Table 2).

As a secondary photochemical pollutant, ozone also is dependent on meteorology in complex ways [*Cox and Chu*, 1996; *Duenas et al*., 2002]. For instance, through alteration of hydroxyl (OH) radical concentrations, the moisture content in air is able to influence ozone chemistry, where wetter conditions tend to reduce ozone while drier conditions tend to favor ozone formation [*Klonecki and Levy*, 1997; *Lelieveld and Crutzen*, 1990; *Murazaki and Hess*, 2006]. Clouds may also significantly reduce photochemical processes vital for surface ozone production [*Flynn et al*., 2010; *Lelieveld and Crutzen*, 1990; *Thompson*, 1984]. Air temperature is typically cited as one of the closest direct associates with boundary layer ozone because it affects rates of photolytic chemistry and also reflects the amount of surface radiation [*Aw and Kleeman*, 2003; *Klonecki and Levy*, 1997; *Sillman and Samson*, 1995]. Calm conditions are typically more advantageous for ozone build up as O_3 is not being removed from the location where it has formed; however, ozone advection and transport from the free troposphere may

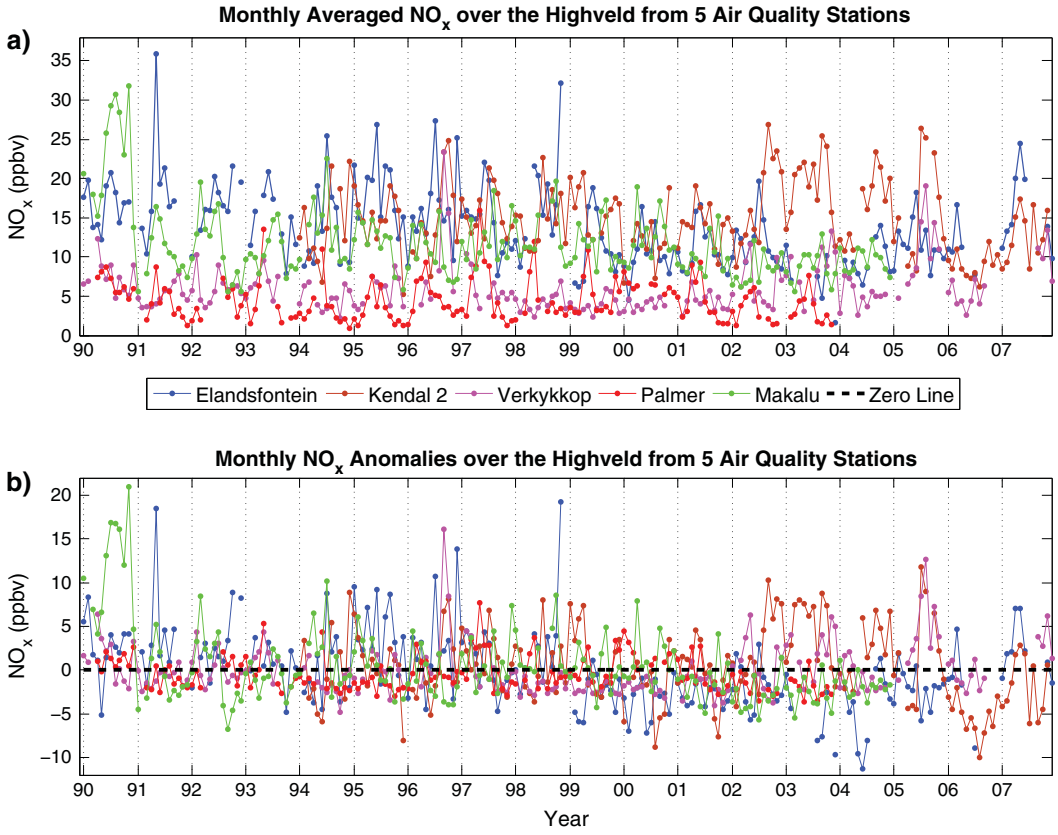

Figure 3. (a) Eighteen years (1990–2007) of monthly NO_x averages (calculated from diurnal 1100–1600 local time averages) over the Highveld and (b) corresponding monthly NO_x anomalies.

present exceptions to this rule [*Tu et al.*, 2007]. In summary, there is ample evidence for a strong relationship between meteorology and the formation of surface ozone. Therefore, if a region is prone to a high frequency of anomalous weather conditions, the surface ozone record should at least partially reflect this variability.

The Highveld presents a good example of such a region. Located at the subsiding edge of Southern Hadley and Ferrel cells, eastern South Africa, where the Highveld is located, generally experiences mean anticyclonic circulation throughout the year. As the circumpolar vortex strengthens in the winter, westerlies expand, forcing the semipermanent high pressure northwestward over the southeastern part of African continent. The resulting synoptic regime generates stable, sunny, and cloudless conditions in the region for most of austral winter from May to September. Starting in October as heating intensifies, westerlies weaken, allowing for the easterlies to expand southward, leading to occurrences of easterly waves and lows. These conditions bring precipitation and clouds to the region, peaking between December and February and lasting approximately until end of April [*Tyson and Preston-Whyte*, 2000]. Year-to-year variability in synoptic patterns over the eastern South Africa, however, can be substantial due to the apparent teleconnection of local meteorology with sea surface temperature (SST) anomalies of the Atlantic, Pacific, and Indian Oceans [*Goddard and Graham*, 1999; *Reason and Jagadheesha*, 2005].

Of the bodies of water mentioned, the tropical Pacific and central Indian Oceans have the greatest importance for modifying normal patterns of weather variability over the Highveld [*Goddard and Graham*, 1999]. SST and pressure variations in the tropical Pacific are normally classified as ENSO (El Niño–Southern Oscillation) or El Niño/La Niña–Southern Oscillation, where generally El Niño refers to *positive* tropical central Pacific SST anomalies and La Niña refers to *negative* tropical central Pacific SST anomalies [*Trenberth*, 1997]. Studies have shown a strong relationship between ENSO and summer-autumn precipitation, temperature, and wind fields over eastern South Africa where usually El Niño is associated with warm and dry conditions while La Niña is accompanied by cool and wet weather [*Lindesay*, 1988; *Tyson*, 1986, chapter 8]. It has also been argued that the influence of Indian Ocean SSTs on precipitation in the region is significant [*Goddard and Graham*, 1999]. Thus, it seems reasonable to expect that both oceans influence rainfall over the Highveld and

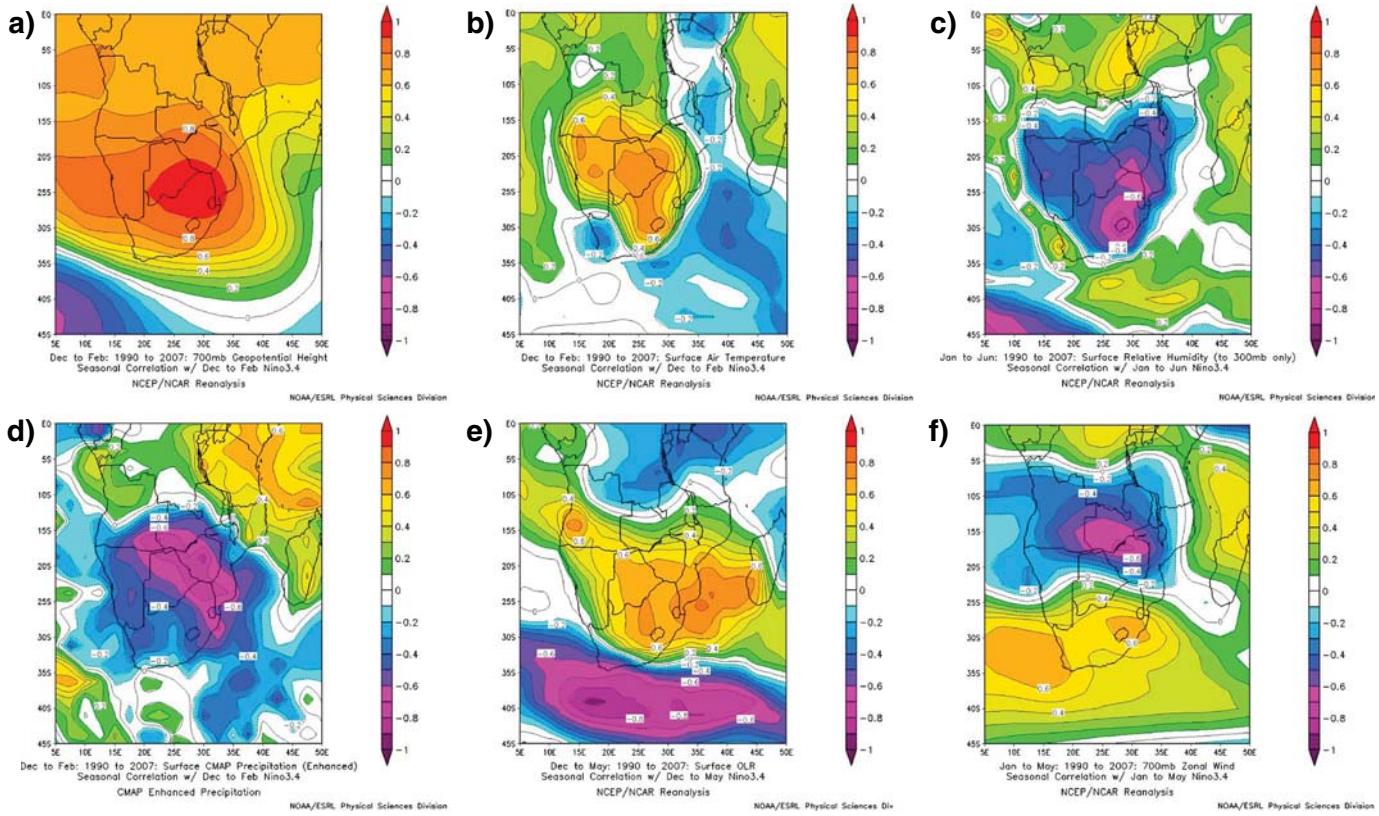

Figure 4. Linear seasonal correlations between six meteorological variables and Niño 3.4 over southern Africa during teleconnection-sensitive months from 1990 to 2007. Each panel corresponds to different meteorological variables: (a) 700 hPa geopotential height, (b) surface air temperature, (c) surface relative humidity, (d) surface CMAP precipitation, (e) outgoing long-wave radiation, and (f) 700 hPa zonal wind. Image provided by the NOAA-ESRL Physical Sciences Division, Boulder Colorado from their Web site at http://www.esrl.noaa.gov/psd/.

perhaps other weather variables, either directly or indirectly, or both. Effects of the ENSO on air flow in the region are extensively discussed in *Kanyanga* [2009]. Linear correlations between Niño 3.4 (one of the ENSO indices) and major meteorological variables from NCEP/NCAR reanalysis [*Kalnay et al*., 1996] and CMAP [CPC (Climate Prediction Center) Merged Analysis of Precipitation] enhanced precipitation [*Xie and Arkin*, 1996] data sets likewise suggest a strong relation between ENSO and local meteorology (Figure 4). Recent research has shown that ENSO may affect free tropospheric ozone by causing changes in large-scale convection and circulation [*Doherty et al*., 2006; *Thompson et al*., 2001].

The main aim of this study is to understand to what extent meteorological variability, as signified by ENSO, and NO_x, as representative of chemical variability, influence seasonal surface ozone concentrations over the South African Highveld. A second objective is to calculate surface ozone trends for the region over the 18 years examined. Figure 5 summarizes a number of pathways by which the weather may influence formation of lower tropospheric ozone. Climate regimes that are thought to influence meteorology of the Highveld are at the top of the diagram. ENSO influences Indian Ocean SSTs and positions of the Walker Circulation. Atlantic Ocean SSTs, the Antarctic Oscillation (AAO), and perhaps other climate modes may play a role in eastern South African weather variability, but these effects are thought to be less important than tropical Pacific and Indian Ocean SSTs. In Figure 5, these climate oscillations appear in the dashed orange box; the affected meteorological parameters over the Highveld are displayed in the dashed blue box. The green dashed box shows ozone precursors, and the black dashed box denotes various sources of NO_x and VOCs. The interaction between ozone precursors (green dashed box) and meteorology (blue dashed box) essentially determines the amount of surface ozone created. Temperature affects the rates of ozone producing reactions. Precipitation can reduce NO_x amounts through the process of wet deposition [*Seinfeld and Pandis*, 2006, pp. 224–227]. Water vapor impacts the oxidation of NO_x and VOCs [*Thompson*, 1992]. Clouds have a significant influence on solar radiation needed to photo dissociate NO_2 leading to ozone formation. Air flow can bring or remove NO_x,

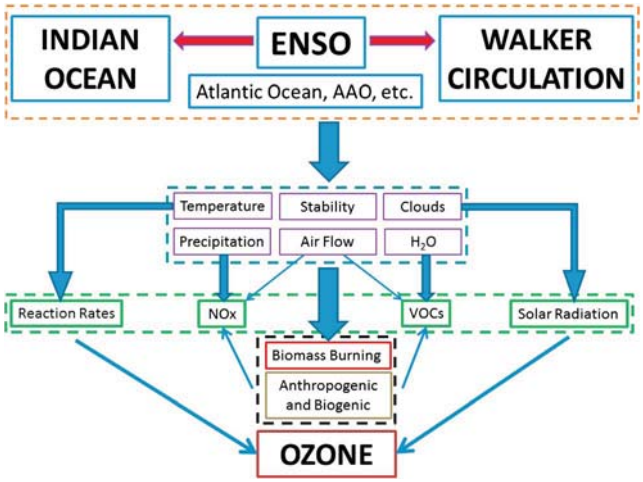

Figure 5. A diagram indicating multicomponent pathways for ENSO to influence ozone over the Highveld. ENSO affects the Indian Ocean and Walker Circulation. These factors along with the other climate regimes such as Antarctic Oscillation (AAO), Atlantic Ocean SSTs, etc. (not considered in this study) potentially affect oscillations (or variability) in eastern South African meteorology. Meteorology perturbations may then affect chemistry required for the surface ozone production, modulating surface ozone amounts over the Highveld.

VOCs, and O_3. Atmospheric stability determines the extent to which ozone precursors can accumulate in the atmosphere. Thus, *La Niña* years experiencing anomalously wet, cloudy, and cool summers should observe a drop in seasonal ozone, whereas *El Niño* years, tending to be comparatively drier, clearer, and warmer in summers, should exhibit a rise in seasonal ozone. Given the pathways above, it is reasonable to expect that at a least partial relationship exists between tropical Pacific SSTs and seasonal surface ozone amounts over the Highveld. We will examine this hypothesis using data from five monitoring stations over the Highveld with a multivariate regression model.

2. Analysis Methods

2.1. Data

We use O_3 and NO_x measurements from five Eskom air quality monitoring stations, namely, Elandsfontein, Kendal 2, Palmer, Verkykkop, and Makalu (Figure 1). Eskom is the power utility in South Africa responsible for the supply of electricity to the country, as well as for funding and maintaining of monitoring stations that were set up in strategic locations in the 1980s and 1990s [*ESKOM*, 2000]. These stations are sited with different objectives: to measure the direct impact of power station plumes (Kendal 2), regional influence of emissions from power stations and industries on the Highveld (Elandsfontein, Verkykkop, Makalu), or upwind conditions (Palmer). In addition to coal-fired power plants, petrochemical and metallurgical industries, other anthropogenic and biogenic sources may significantly affect the concentrations of local NO_x and other ozone precursors near each station. In our analysis, only measurements taken during local 1100–1600 h are used to produce daily and monthly averages of ozone and NO_x. This allows us to characterize the composition of the well-mixed daytime atmospheric boundary layer and to avoid complexities of the nighttime chemistry and boundary layer dynamics [*Cooper et al.*, 2012]. The monthly averaged value is also based on a criterion of having at least 75 h of data (about a third of a month).

Table 1 summarizes some technical aspects of the mentioned air quality monitoring stations. The gas analyzers utilized to measure ozone and NO_x were all US-EPA approved equivalent and reference methods, respectively. Detailed records of instrument calibration and zero and span checks exist and have been used to assess the data quality for the measurement period by Eskom measurement specialists. *Elandsfontein* is located 25 km east of the Kriel and Matla Power Stations and 50 km south-southeast of eMalahleni (previously Witbank) in central Mpumalanga. The site is surrounded by coal mining and other industries, low income townships, and motor vehicle emission sources. *Kendal* 2 is located 2 km south-southeast (downwind) of the Kendal Power Station [*Rorich and Galpin*, 1998]. The station is close to direct pollution sources and at times exhibits chaotic diurnal or weekly behavior depending on exposure to pollution plumes. Nevertheless, it is expected to be sensitive to meteorology on longer seasonal scales [*Thomas and Scorgie*, 2006]. *Verkykkop* is positioned 10 km north of the town of Volksrust and 35 km away from the nearest power plant [*Mokgathle*, 2006]. *Palmer* is within an approximately 20 km radius of three towns; the major power plants are to the southwest and usually downwind [*Rorich and Galpin*, 1998]. Finally, *Makalu* is situated in agricultural farmlands and is generally a rural station. Other times, because it is 5 km east of the Sasolburg industrial area and 12 km south-southwest of the Lethabo Power Station, it is exposed to industrial emissions [*Rorich and Galpin*, 1998].

In the Highveld, the relationship between ozone and NO_x is complex, as illustrated in Figure 6, where ozone is plotted versus NO_x. The scatter plots are divided into early and later time segments.

Table 1. Details of Eskom Ambient Air Quality Monitoring

Monitoring Station	Elandsfontein	Kendal 2	Verkykkop	Palmer	Makalu
Site description	A regional monitoring station situated in the middle of the industrialized Highveld and impacted by a multitude of sources	Immediately downwind of a large power station, in the zone of maximum ground-level impact	A regional air quality monitoring station situated downwind of the industrialized Highveld (the nearest large power station is 27 km away)	Situated in eastern Mpumalanga, upwind of the industrialized Highveld and adjacent to the escarpment	Situated in the northern Free State, with occasional influence from industries to the west and north
Coordinates	Latitude: −26.25 Longitude: 29.41	Latitude: −26.08 Longitude: 28.96	Latitude: −27.31 Longitude: 29.88	Latitude: −25.51 Longitude: 30.06	Latitude: −26.83 Longitude: 27.90
Altitude (m)	~1600	~1550	~1700	~1800	~1450
Time period data available	1990–2007	1994–2007	1990–2007	1990–2003	1990–2004
Calibration procedure and frequency	Dynamic multipoint (at a minimum zero/span and three intermediate point checks) calibrations are conducted on site at least quarterly against an accurate known gas standards and an ozone primary standard Two-weekly zero/span checks against accurate known gas standards and an ozone primary standard				
Calibration standards	Eskom Calibration Laboratory (South African National Accreditation System (SANAS) Laboratory Number: 1503)				
Gas analyzers	Continuous UV Photometric Ozone analyzers, (manufacturers: Monitor Labs, Thermo Environment Instruments/Electron (US-EPA EQOA-0880-047), and Dasibi) Continuous $NO/NO_2/NO_x$ chemiluminescence technology (manufacturers: Monitor Labs, Thermo Environmental Instruments/ Electron $NO\text{-}NO_2\text{-}NO_x$ (US-EPA RFNA-1289-074)				

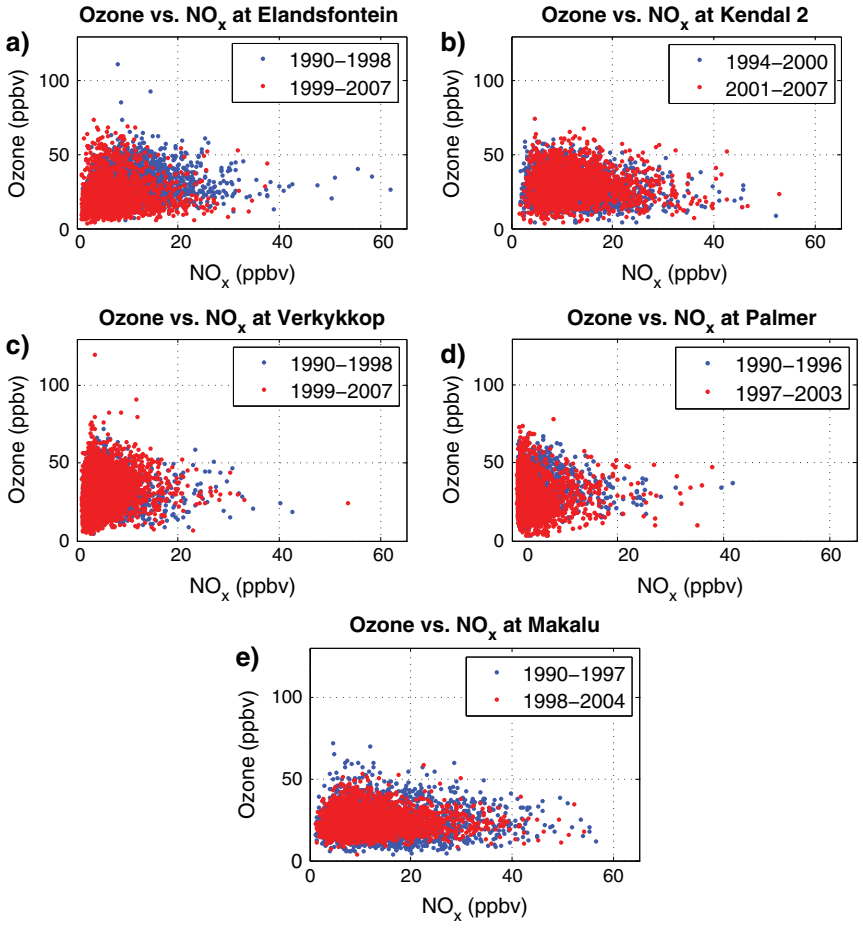

Figure 6. Daily averaged (1100–1600 local time) ozone versus NO_x mixing ratios for the first half of the data set studied (blue) and the second half (red) at (a) Elandsfontein, (b) Kendal 2, (c) Verkykkop, (d) Palmer, and (e) Makalu.

Table 2. Summary of Statistics Applied to Daily Averages of Ozone/NO_x, Ozone, and the NO_x Time Series Shown in Figure 6, Where Bold Marks a Later Period

		Ozone/NO_x	Ozone	NO_x
	Elandsfontein			
Early period (1990–1998)	Mean	3.74	29.58	10.61
	Standard deviation	2.48	10.28	6.32
Late period (1999–2007)	Mean	**4.49**	**21.89**	**7.29**
	Standard deviation	**3.86**	**10.59**	**5.10**
T test	Significant at 95 %?	Yes	Yes	Yes
	P value	0.00	0.00	0.00
	Kendal 2			
Early period (1994–2000)	Mean	3.25	27.13	11.62
	Standard Deviation	2.40	9.56	6.49
Late period (2001–2007)	Mean	**3.09**	**29.53**	**12.21**
	Standard Deviation	**2.03**	**10.59**	**6.72**
T test	Significant at 95 %?	Yes	Yes	Yes
	P value	0.02	0.00	0.00
	Verkykkop			
Early period (1990–1998)	Mean	8.10	31.14	5.57
	Standard deviation	5.10	10.53	4.17
Late period (1999–2007)	Mean	**8.17**	**30.83**	**5.59**
	Standard deviation	**5.98**	**12.72**	**4.27**
T test	Significant at 95%?	No	No	No
	P value	0.65	0.31	0.85
	Palmer			
Early Period (1990–1996)	Mean	11.38	33.38	4.38
	Standard deviation	7.20	10.87	4.01
Late Period (1997–2003)	Mean	**11.31**	**29.89**	**4.33**
	Standard deviation	**8.77**	**12.04**	**4.09**
T test	Significant at 95%?	No	Yes	No
	P value	0.77	0.00	0.71
	Makalu			
Early period (1990–1997)	Mean	2.42	24.07	14.35
	Standard deviation	2.02	8.55	9.23
Late period (1998–2004)	Mean	**2.81**	**24.52**	**12.31**
	Standard deviation	**2.03**	**7.22**	**7.56**
T test	Significant at 95%?	Yes	No	Yes
	P value	0.00	0.06	0.00

Table 2 compares these time periods by indicating their mean, standard deviation, and whether the two periods are statistically different. For Elandsfontein and Kendal 2 (Figures 6a and 6b), statistically significant change is observed in the ozone and NO_x values over the two segments. This is not surprising as both of these sites are located between the industrialized Gauteng and power plants (see Figure 1). Being somewhat removed from emission sources, Verkykkop and Palmer (Figures 6c and 6d) mostly exhibit no statistical change in ozone and NO_x values over the two periods (Table 2). Also, NO_x values at these two stations are noticeably lower than at all other stations (Figure 3a and Table 2). The Makalu station (Figure 6e and Table 2) tends to have a substantially different ozone-NO_x behavior compared to the other four stations, where on many occasions ozone is comparatively low when NO_x is relatively high.

Meteorological data are provided by the South African Weather Service from the Irene weather station located near Pretoria (Figure 1). Variables obtained are near-surface values of temperature in Celsius, relative humidity in percent, precipitation in millimeters, and cloud cover in total cloud octas where the observations are taken three times a day: 0800, 1400, and 2000 local time. We average all three readings to obtain an average cloud cover for a single day. Temperature and cloud cover data are available for the 18 years (1990–2007), relative humidity data begins in 1992, and precipitation measurements only start in 1993.

Table 3. El Niño and La Niña Events as Classified by ONI During the 1990–2007 Period With Strongest Episodes Marked in Bold

Events	Period
El Niño	**1991 AMJ–1992 JJA**, 1994 AMJ–1995 FMA, **1997 AMJ–1998 AMJ**, 2002AMJ–2003 FMA, 2004 MJJ–2005 JFM, 2006 JAS–2007 DJF
La Niña	1995 ASO–1996 FMA, **1998 JJA–2000 MJJ**, 2000 SON–2001 JFM, 2007 ASO–2008 AMJ

2.2. Regression Model

One way to identify a signal such as ENSO in surface ozone data is to use a generalized regression model similar to the one described in *Ziemke et al*. [1997] [see also *Bloomfield et al*., 1996; *Randel and Cobb*, 1994; *Stolarski et al*., 1991]. Such a model assumes a linear relationship between the variable in question and selected predictors as a first approximation of the problem. In our case, the expected predictors are time, ENSO index, and 3 month moving averaged NO_x anomalies leading to the following four equations:

$$\hat{T}(t) = \alpha + \beta \cdot t + \epsilon(t) \tag{1}$$

$$\hat{T}(t) = \alpha + \beta \cdot t + \gamma \cdot \mathrm{ENSO}(t) + \epsilon(t) \tag{2}$$

$$\hat{T}(t) = \alpha + \beta \cdot t + \delta \cdot \mathrm{NO}_x(t) + \epsilon(t) \tag{3}$$

$$\hat{T}(t) = \alpha + \beta \cdot t + \gamma \cdot \mathrm{ENSO}(t) + \delta \cdot \mathrm{NO}_x(t) + \epsilon(t) \tag{4}$$

where α is seasonal fit, β is trend coefficient, t is time, γ is the regression coefficient for the time series ENSO(t), and δ is the regression coefficient for the time series NO_x(t). Finally, ϵ(t) is the residual that is calculated by subtracting the modeled time series $\hat{T}(t)$ from the actual observed time series $T(t)$. Time t is the first predictor, time series ENSO(t) is the second predictor, and the time series NO_x(t) is the third predictor. Because the variables of interest exhibit strong seasonal variability, each regression parameter is presented by a cosine and sine harmonic expansion with α employing four harmonics—12 month, 6 month, 4 month, and 3 month—and other coefficients employing three harmonics—12 month, 6 month, and 4 month. For example, α expansion with A, B, and C being constants can be written as following:

$$\alpha = A + \sum_{k=1}^{\text{harmonics}=4} \left[B_k \cos\left(\frac{2\pi\, kt}{12}\right) + C_k \sin\left(\frac{2\pi\, kt}{12}\right) \right]. \tag{5}$$

A similar procedure is carried out for the other regression coefficients. In order to calculate these coefficients, this model uses the least squares estimates method [*Bloomfield*, 2000, Chapter 2; *Wilks*, 2011, Chapter 9].

It is common practice to use the Oceanic Niño Index (ONI) to study ENSO impacts on meteorology over eastern South Africa; this has been done for precipitation and air transport anomalies [*Kanyanga*, 2009; *Landman et al*., 2012]. ONI is an ENSO operational index used by National Oceanic and Atmospheric Administration (NOAA) that is defined as a 3 month moving average of the SST anomalies from 1971–2000 climatology in the 3.4 Niño region located in the equatorial Pacific Ocean. An event is classified as El Niño if the 3 month SST anomaly mean exceeds +0.5 °C for five consecutive months, while La Niña conditions require 3 month SST anomaly mean to persist below −0.5 °C for five consecutive months (ONI; http://www.cgd.ucar.edu/cas/ENSO/enso.html). Table 3 specifies which years from 1990 to 2007 are categorized as El Niño events and which years are categorized as La Niña events according to ONI. The typical way to represent t is in months; however, for consistency with the ONI proxy, the time series is smoothed by 3 month moving averages.

We are interested in determining whether adding parameters to our model such as ENSO and NO_x improves the observed data fits; therefore, we determine adjusted coefficients of determination for each time we run the model. The adjusted coefficient of determination, R_a^2, establishes how well a model fits the data with the added independent variables. It is determined in the following way:

$$R_a^2 = 1 - \left(\frac{n-1}{n-p}\right) \frac{\sum \left(T_i - \hat{T}_i\right)^2}{\sum \left(T_i - \overline{T}\right)^2} \tag{6}$$

where $\overline{T}$ is an average of time series, p is a number of coefficients used, and n is a sample size. In order to estimate an error of calculated parameters, we employ a bootstrap resampling technique where residuals are

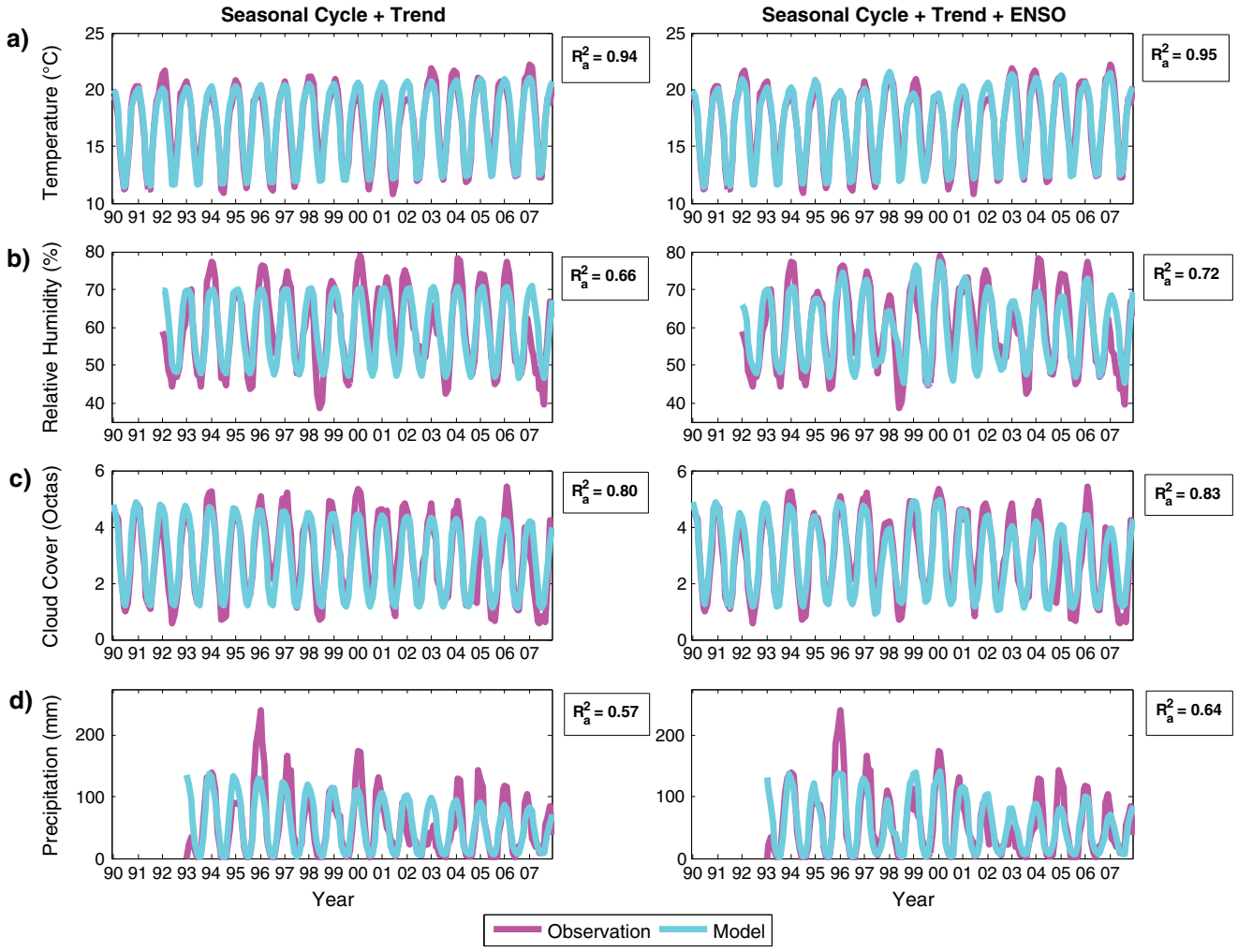

Figure 7. Comparison of observed meteorological variables at Irene with two model fits to those variables: two parameter model and three parameter model. Each row corresponds to a single variable: (a) temperature, (b) relative humidity, (c) cloud cover, and (d) precipitation.

resampled generating 10,000 new time series while keeping predictors fixed [*Efron and Tibshirani*, 1993; *Freedman*, 1981]. Since this method is only valid for independent data, we use moving-blocks bootstrap when resampling our residuals to account for autocorrelation in the time series [*Wilks*, 1997]. After these procedures, we are left with a distribution of 10000 coefficients from which we can determine the standard deviation of any desired parameter [*Higgins*, 2003].

3. Results

3.1. ENSO and Meteorology Over the Highveld

We are interested in quantifying effects of ENSO on surface ozone and some chemistry-affecting meteorology over the Highveld from 1990 to 2007. In this section, we apply the regression equations (1) and (2) to four meteorological fields at Irene: temperature, relative humidity, cloud cover, and precipitation (we do not expect NO_x to have any effect on meteorology). First, we use only two parameters in our model: the seasonal cycle and trend. Then we employ three parameters, where the ENSO term is added to seasonal cycle and trend terms. Afterward we are able to compare two cases and see what effect, if any, ENSO has on meteorology over the Highveld (Figure 7). Applying equation (1) for all four weather variables results in generally high coefficients of determination. The model is able to reproduce 94% of temperature variability (Figure 7a) over the 1990–2007 period. Precipitation is less consistent, so only 57% of variability (Figure 7d) is explained by equation (1). The reason for these relatively high R_a^2 values is the well-defined seasonality of eastern South Africa with clear wet

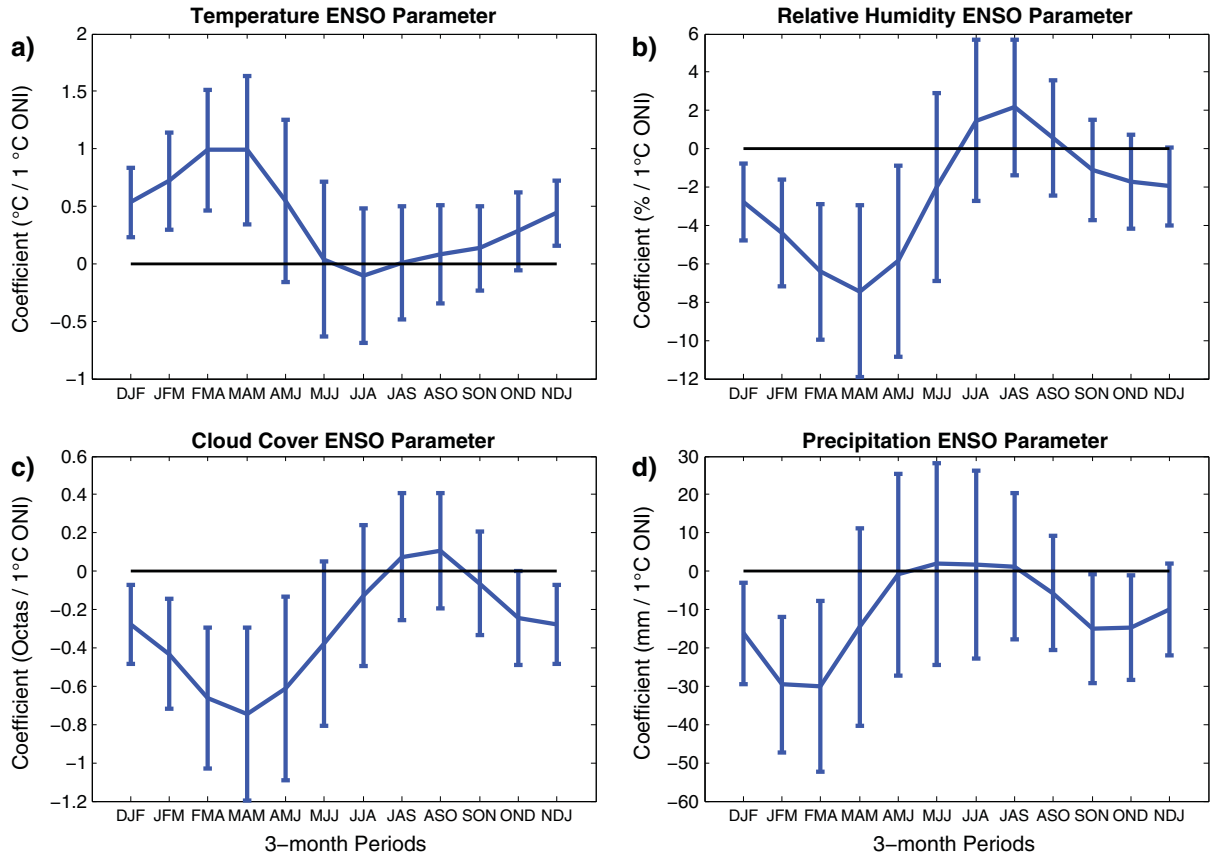

Figure 8. ENSO coefficients derived by the model for the four Irene meteorological variables: (a) temperature ENSO coefficient, (b) relative humidity ENSO coefficient, (c) cloud cover ENSO coefficient, and (d) precipitation ENSO coefficient. Zero line is indicated in black.

and dry periods; this allows the seasonal cycle term in the model to explain significant portion of each meteorological variable considered. Thus, when we add an ENSO parameter, there are only slight increases in R_a^2 values for all of the meteorological variables.

ENSO parameters for the weather variables indicate the calculated seasonal ENSO effect on each of the variables using equation (2) (Figure 8). An ENSO parameter is grouped into 12 3 month moving average periods or 12 smoothed monthly averages (DJF $= \widetilde{J}$, JFM $= \widetilde{F}$, etc.) such that each smoothed month has its own sensitivity toward the ENSO time series. A coefficient (parameter) tells us how many units of a variable are changed by the one unit of ONI (1 °C SST anomaly of the Pacific Ocean region Niño 3.4). In order for the coefficient to be significant at the 0.05 α level, it is necessary for an error bar not to touch or cross the zero line, in other words to be significantly different from zero. For temperature (Figure 8a), smoothed January (from now on just month name) has an ENSO coefficient of approximately 0.5 °C per one unit of ONI. The coefficient is largest for March and April, where we see 1 °C per 1 ONI, although the effect is still significant from December to April. For June through October, the effects of ENSO are insignificant. Thus, even though the October response is positive, we cannot ascertain its robustness because of the uncertainty in calculating the regression coefficient. For relative humidity (Figure 8b), an opposite effect of ENSO compared to temperature is observed in January–March. The maximum drop occurs in April where about 7% of the relative humidity is reduced per ONI. The cloud cover ENSO coefficient (Figure 8c) generally follows the relative humidity sensitivity toward ENSO, but with a few minor differences. April for cloud cover exhibits a minimum with 0.7 octas reduced per 1 ONI; however, the effect is still statistically significant in May. Precipitation (Figure 8d) decreases with the largest rate of 30 mm per ONI in February and March. Smaller but significant reductions in precipitation are evident in January, October, and November.

In summary, meteorology, expressed in the four variables examined, is primarily sensitive toward the wet season ENSO events starting in November until about May. Temperature, humidity, and cloud cover appear

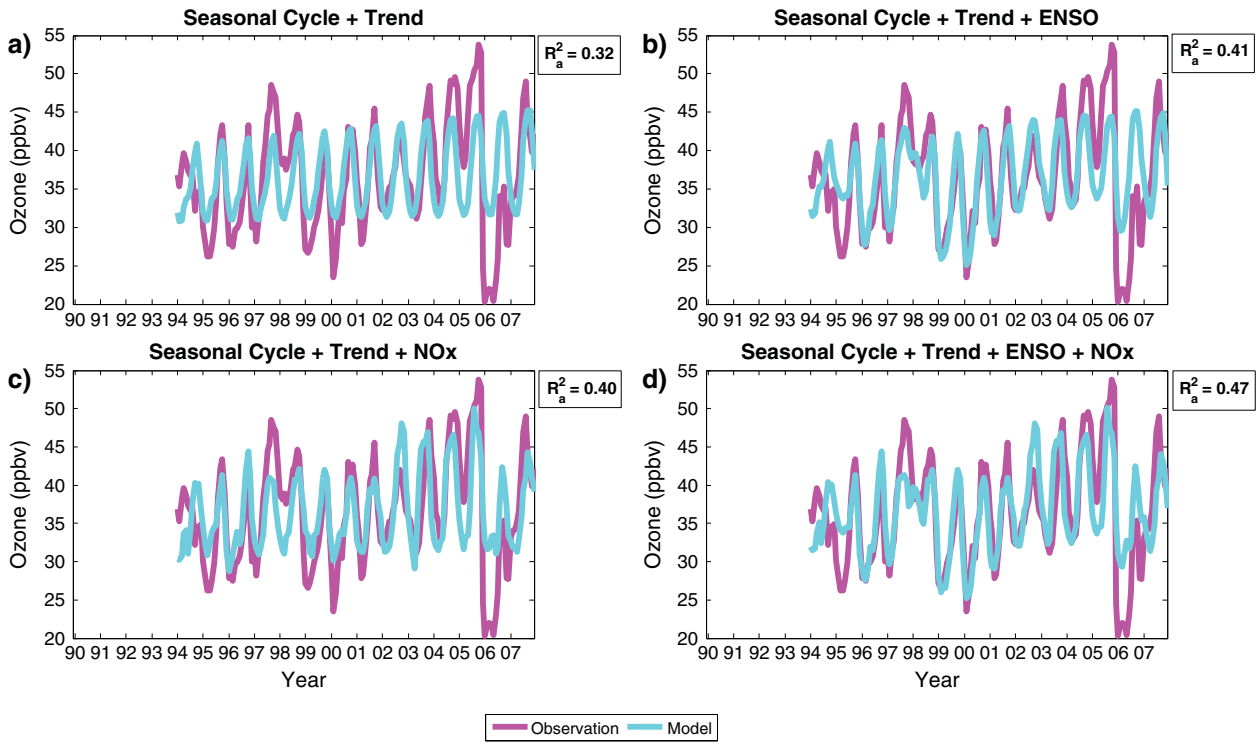

Figure 9. Comparison of the 3 month moving average surface ozone at Kendal 2 with the four model fits to this surface ozone data. Each of the four model fits uses different combinations of the parameters: (a) Seasonal Cycle + Trend, (b) Seasonal Cycle + Trend + ENSO, (c) Seasonal Cycle + Trend + NO_x, and (d) Seasonal Cycle + Trend + ENSO + NO_x.

to vary with Pacific Ocean temperature more smoothly than precipitation, with cloud cover extending its significant response as far as May. In the next section, we discuss our results regarding the dependency of surface ozone over the Highveld on ENSO and NO_x.

3.2. ENSO, NO_x, and Surface Ozone at the Highveld

To understand the nature of surface ozone variability over the Highveld, we apply equations (1)–(4) to each of the five air quality monitoring stations and determine adjusted coefficients of determination, respectively. This method allows us to compare four different fits and see if our predictors, ENSO and NO_x, help us to describe observed surface ozone time series more accurately than seasonality and trends alone. Figure 9 shows this analysis graphically for Kendal 2 station. When the model uses seasonal cycle and trend terms, the observations are reproduced reasonably well, partially because ozone fluctuations exhibit pronounced seasonality (Figure 9a; $R_a^2 = 0.32$). We do, however, notice that yearly minima and maxima values are not well represented by the model with just two parameters. If we add an ENSO term ,then the 1996–2001, 2005, and 2006 ozone minima fits noticeably improve (Figure 9b; $R_a^2 = 0.41$). Adding a NO_x term without an ENSO term also helps our fit slightly with 1996, 2003–2005, and 2006 maxima (Figure 9c; $R_a^2 = 0.40$). Using all four terms in this case gives us an overall best fit, with the highest adjusted coefficient of determination (Figure 9d; $R_a^2 = 0.47$). It is important to notice that even though on the whole our fit improves, at certain times the fit gets worse. In the example of Kendal 2, maxima for 2000 and 2001 are represented less accurately with all of the four parameters than just with two parameters and ENSO. A similar procedure is carried out for the other four stations (Figure 10). The corresponding adjusted coefficients of determination are summarized in Table 4, where the best model fits are marked in bold.

Figure 10 compares the two parameter model and the best fit model for each of the stations. Elandsfontein (Figure 10a) does not exhibit consistent ozone seasonality; therefore, the model with two parameters simulates the observed time series rather poorly. Adding ENSO and NO_x terms sheds some light on large-scale features of ozone variability. For instance, an ozone increase in 1998 and subsequent ozone fall in 1999

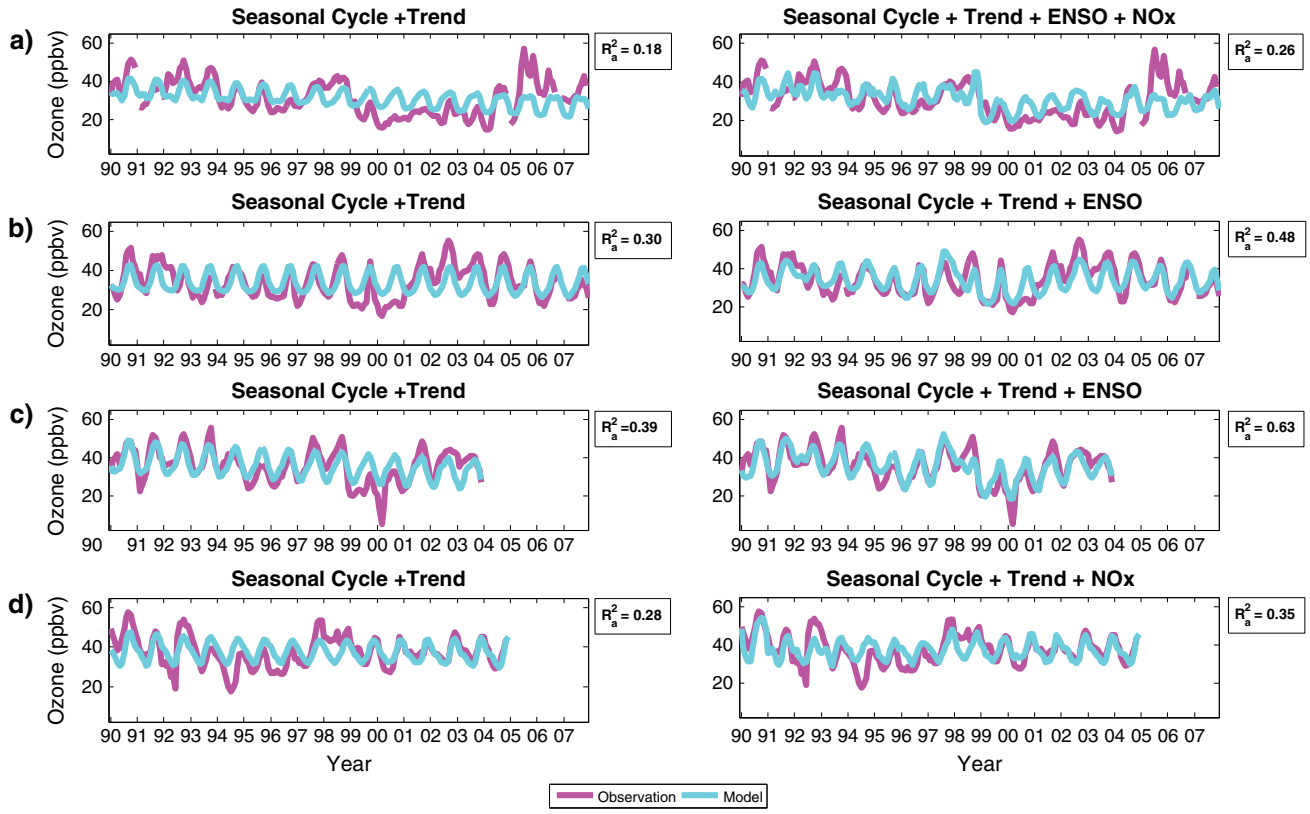

Figure 10. Comparison of the 3 month moving average surface ozone at each of the four air quality stations with two parameter model fits and the best model fits. Each row corresponds to an air quality station: (a) Elandsfontein, (b) Verkykkop, (c) Palmer, and (d) Makalu.

are well reproduced by the model although peaks in 1998 and 2000 are not well matched. A large error occurs in 2005, where two large peaks are observed, but the model completely fails to indicate large magnitudes. Even though details are not precise, the overall shape of the time series is discernible from the four parameter model at Elandsfontein. Furthermore, the adjusted coefficient of determination has increased from 0.18 to 0.26 with the two additional factors. For Verkykkop (Figure 10b), the NO_x term does not help the fit (not shown) and actually slightly reduces overall model accuracy. The three parameter model, where the third parameter is ENSO, gives the best improvement over the two parameter model. This station has a clear seasonality, but adding an ENSO term increases model accuracy significantly (from $R_a^2 = 0.30$ to $R_a^2 = 0.48$). Minima in 1992, 1996, 1999, and 2000 are now better matched by the model. Relatively smaller improvements in ozone peaks are observed for 1991, 1995, and 2002. Palmer station (Figure 10c) also has a strong seasonal ozone cycle. Similar to Verkykkop, the NO_x term does not help in improving the accuracy of our model; therefore, we use the three parameter model as for Verkykkop. The ENSO term improves the model fit significantly and has the highest adjusted coefficient of determination among all of the examined stations of 0.63. The major improvements are seen in the ozone maximum of 1997 and the ozone minima of 1999 and 2000. The last station, Makalu (Figure 10d), is not sensitive to

Table 4. Coefficients of Determination for Each of the Stations With All Four Combinations of the Parameters Where Highest R_a^2 Are Marked in Bold Corresponding to the Best Model Fit at a Particular Location

	$\alpha+\beta$	$\alpha+\beta+\gamma$	$\alpha+\beta+\delta$	$\alpha+\beta+\gamma+\delta$
Elandsfontein	0.18	0.21	0.22	**0.26**
Kendal 2	0.32	0.41	0.40	**0.47**
Verkykkop	0.30	**0.48**	0.29	0.47
Palmer	0.39	**0.63**	0.42	0.62
Makalu	0.28	0.26	**0.35**	0.34

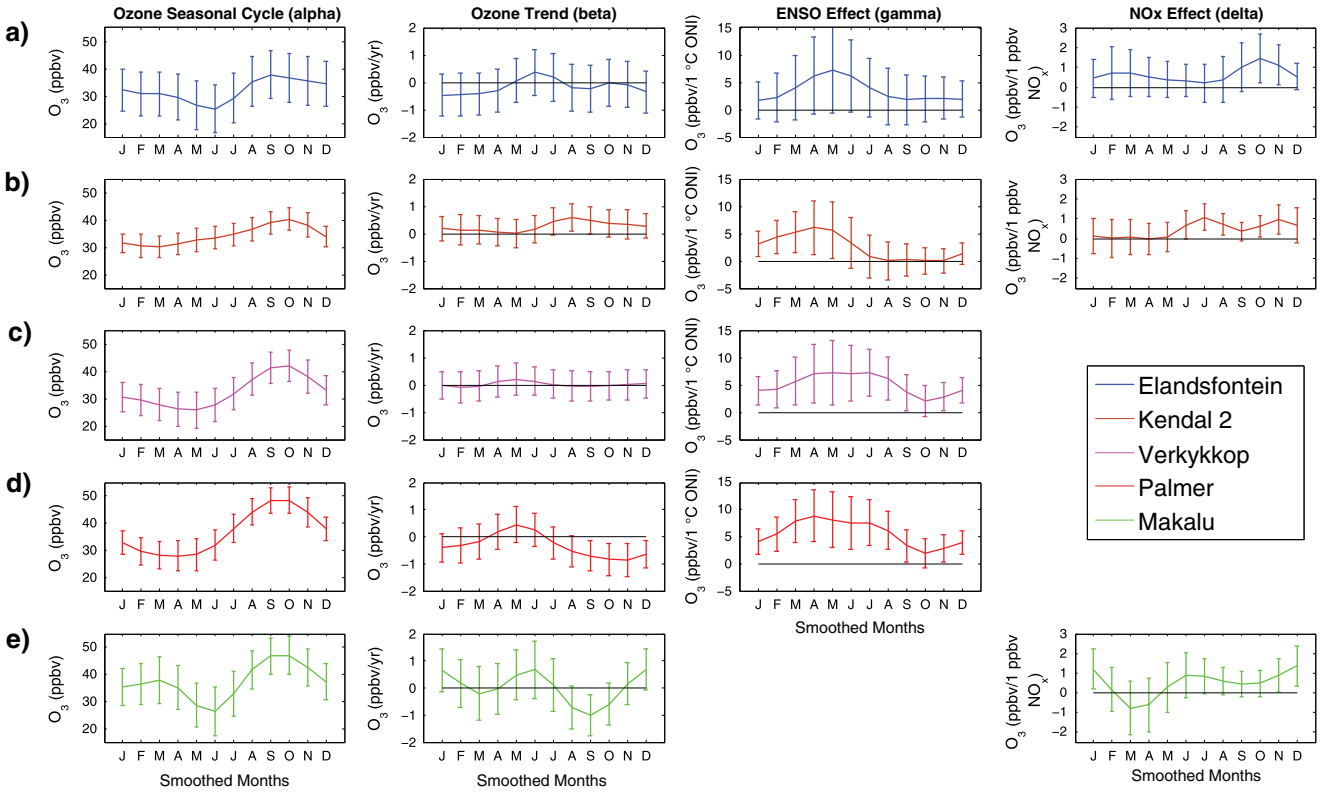

Figure 11. Monthly (smoothed months) contributions of each parameter to the best model fits for each of the five stations: (a) Elandsfontein, (b) Kendal 2, (c) Verykykop, (d) Palmer, and (e) Makalu. Zero line is indicated in black.

ENSO and only improves when we apply the three parameter model adding the NO_x term. The model accuracy is not bad because Makalu observations exhibit a regular yearly ozone cycle. However, lack of relationship to ENSO variability implies that Makalu station may be exposed to an environment different from the other four stations.

To estimate ENSO and NO_x impacts on surface ozone over the Highveld, we examine coefficients for all of the parameters that went into the best model fit for each of the five aforementioned stations (Figure 11). According to the model, the seasonal ozone cycle at Elandsfontein (Figure 11a) has a minimum in early winter and maximum in early spring. An ozone trend is not statistically significant over the 18 years studied. ENSO effects are not significant; however, as we previously noted, the ENSO helps slightly with the fit of the model. The NO_x effect is generally important in winter and spring. The seasonal cycle at Kendal 2 (Figure 11b) has a minimum in late summer and a maximum in early spring. Except for a positive ozone trend in August of about 0.4 ppbv per year, no statistically significant trend is found. ENSO influence is evident from January to May with maximum in April of about 6 ppbv per ONI. NO_x is seen to affect parts of winter and parts of spring. At Verykykop (Figure 11c), the seasonal cycle is minimum in autumn and maximum in spring. There is no statistically significant trend in any of the months. The ENSO effect in Verykykop peaks during April–July with a magnitude of approximately 7 ppbv per ONI and is statistically significant for all months of the year except October. Similar to Verykykop, Palmer (Figure 11d) exhibits an ozone minimum in autumn and ozone maximum in spring. A small but statistically significant negative ozone trend of about 0.5 ppbv per year is observed in spring and early summer. With respect to ENSO, Palmer closely resembles Verykykop with statistically significant ENSO coefficients for all months except October and with a maximum in April of approximately 8 ppbv per ONI. Makalu (Figure 11e) has the lowest ozone in early winter and maximum ozone in spring. The ozone trend is negative for September (1 ppbv per year). NO_x has a slight effect on Makalu ozone in November through January. These results indicate some nonhomogeneity among the stations and support our hypothesis that there are multiple reasons for the large-scale variability of surface ozone over the Highveld.

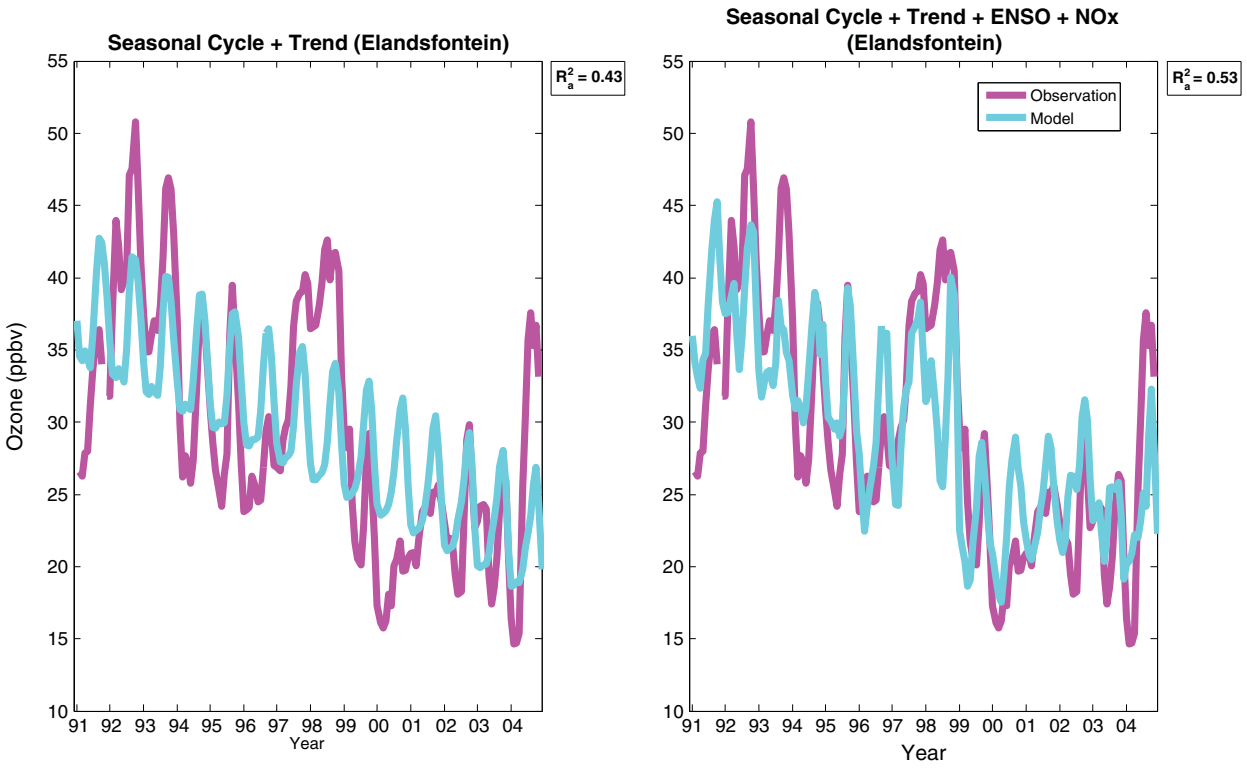

Figure 12. Comparison of the 3 month moving average surface ozone at Elandsfontein with (left) the two parameter model fit and (right) the best model fit using the reduced data set of 1991–2004.

4. Discussion

If ozone time series of all the five stations (Figures 9 and 10) are compared, we observe that Elandsfontein exhibits the greatest irregular variability of surface ozone. The most striking contrast relative to the other stations is evident in the surface ozone seasonal cycle that sometimes is difficult to identify in the Elandsfontein 18 year ozone record, whereas at the other four stations, the annual cycle is almost always visibly present. Large-scale temporal variability is pronounced at Elandsfontein, with a dramatic ozone drop during 1998 and 1999 and a peak in 2005. It is likely that both natural and anthropogenic factors regulate ozone amounts over this location because the model displayed significant NO_x effects on ozone concentrations in spring. Elandsfontein may be influenced by colliery stock piles, coal mine spontaneous combustion, and domestic burning of coal and wood from nearby low income areas. Additional NO_x is transported to the Highveld in spring as the seasonally varying African biomass burning zone propagates southward [*Marufu et al*., 2000]. Fluctuations in regional meteorology may play an important role in controlling local ozone perturbations. In the previous section, we determined that at Elandsfontein ENSO effects on ozone are not significant over any of the months. However, if we rerun our model for Elandsfontein using the time period 1991–2004, to focus only on the stronger ENSO episodes, we observe that the ENSO effect is now significant for November, December, and February through May (not shown), which is more in line with the other three stations. Variations at Elandsfontein are well represented in the shorter-run model, especially the 1998–1999 ozone decrease that is attributed to a NO_x decrease and the strong La Niña of 1998–2000 (Figure 12).

The other stations show more of a pronounced ozone cycle, indicating relative consistency of ozone precursors over time (Figures 9 and 10). Kendal 2, the closest station to Elandsfontein, has a significant NO_x effect on ozone in winter and spring, probably due to biomass burning, domestic fuel use and proximity to numerous industries. The Kendal 2 station is also prone to plumes from the local power station, which at times lead to high NO concentrations and much reduced ozone concentrations [*Collett et al*., 2010]. With regard to ENSO, Kendal 2 resembles the reduced Elandsfontein case with noticeable ozone drops during the 1998–2000 La Niña events. At Makalu, NO_x is found to have an effect on ozone in the November–January period, perhaps

Table 5. Summary of Statistics Applied to Daily Averages of Ozone/NO_x, Ozone, and the NO_x Time Series During El Niño and La Niña Years With Approximate El Niño years—1991, 1992, 1994, 1995, 1997, 1998, 2002, 2003, 2004, 2005, 2006, and 2007—and Approximate La Niña Years—1995, 1996, 1998, 1999, 2000, 2001, and 2007

		Ozone/NO_x	Ozone	NO_x
		Elandsfontein		
La Niña	Mean	3.56	23.41	9.39
	Standard deviation	2.73	10.10	6.42
El Niño	Mean	**4.35**	**27.02**	**9.08**
	Standard deviation	**3.44**	**11.05**	**6.07**
T test	Significant at 95%?	Yes	Yes	No
	P value	0.00	0.00	0.08
		Kendal 2		
La Niña	Mean	3.26	27.29	11.62
	Standard deviation	2.42	9.84	6.45
El Niño	Mean	**3.15**	**29.29**	**12.14**
	Standard deviation	**2.10**	**10.26**	**6.64**
T test	Significant at 95%?	No	Yes	Yes
	P value	0.08	0.00	0.01
		Verkykkop		
La Niña	Mean	7.50	26.03	5.20
	Standard Deviation	4.69	10.21	4.53
El Niño	Mean	**8.47**	**32.72**	**5.62**
	Standard Deviation	**5.55**	**11.41**	**4.05**
T test	Significant at 95 %?	Yes	Yes	Yes
	P value	0.00	0.00	0.00
		Palmer		
La Niña	Mean	9.44	26.86	4.45
	Standard deviation	6.86	11.24	4.05
El Niño	Mean	**13.25**	**33.68**	**3.90**
	Standard deviation	**8.46**	**10.98**	**3.86**
T test	Significant at 95%?	Yes	Yes	Yes
	P value	0.00	0.00	0.00
		Makalu		
La Niña	Mean	2.42	23.31	13.57
	Standard deviation	1.85	7.43	7.88
El Niño	Mean	**2.67**	**24.07**	**12.96**
	Standard deviation	**2.10**	**8.61**	**8.03**
T test	Significant at 95%?	Yes	Yes	Yes
	P value	0.00	0.00	0.01

signifying the impact of local anthropogenic NO_x sources. On the map in Figure 1, it appears that Makalu is located in closer proximity to relatively strong NO_x emission sources than the other stations. Additionally, Figure 6 shows that the NO_x versus ozone relationship at Makalu differs from other stations. These reasons may explain the lack of ozone-to-ENSO relation at Makalu. Verkykkop and Palmer are not sensitive to NO_x anomalies. Both of these locations are somewhat removed from the heaviest industrial zone (Figure 1), indicating that the meteorological variability is of greater prominence than NO_x variability. Therefore, Verkykkop and Palmer experience greater perturbations in surface ozone than other three stations during ENSO events.

Additional analysis on the ozone-NO_x relationship during El Niño and La Niña years appears in Table 5. Table 5 shows basic statistics applied to daily averages of three variables: ozone/NO_x, ozone, and NO_x. At all of the stations, the variables means for El Niño and La Niña, with the exception of NO_x at Elandsfontein and ozone/NO_x at Kendal 2, are statistically different from each other. This is not surprising because meteorology affects both: ozone and NO_x. For all of the stations, the ozone mean during El Niño years is larger than the ozone mean during La Niña years. This is partially explained by the dependence of ozone formation on the meteorological processes.

In Figure 8, we looked at the ENSO coefficients for the four weather variables and concluded that ENSO significantly influences temperature during December–April, relative humidity during January–May,

Table 6. Yearly Ozone Trends (ppbv/yr) for Each of the Five Analyzed Highveld Stations With Trend Values and Their 95% Confidence Limits for All the Seasons and a Combined Value (Significant Trends Are Marked in Bold)

Seasons	Trend ± 95% Confidence Limit (ppbv/yr)
Elandsfontein: 1990–2007	
Spring	−0.11 ± 0.86
Summer	−0.42 ± 0.78
Autumn	−0.23 ± 0.79
Winter	0.12 ± 0.86
All	−0.16 ± 0.82
Kendal 2: 1994–2007	
Spring	0.40 ± 0.52
Summer	0.20 ± 0.48
Autumn	0.07 ± 0.51
Winter	0.40 ± 0.50
All	0.27 ± 0.50
Verkykkop: 1990–2007	
Spring	−0.08 ± 0.54
Summer	−0.06 ± 0.53
Autumn	0.09 ± 0.56
Winter	0.07 ± 0.52
All	0.01 ± 0.54
Palmer: 1990–2003	
Spring	**−0.92 ± 0.65**
Summer	−0.45 ± 0.58
Autumn	0.17 ± 0.66
Winter	−0.21 ± 0.65
All	−0.35 ± 0.64
Makalu: 1990–2004	
Spring	−0.47 ± 0.76
Summer	0.51 ± 0.82
Autumn	0.03 ± 1.05
Winter	0.00 ± 0.96
All	0.02 ± 0.90

cloud cover during December–May, and precipitation during October–November and January–March. It appears that at least for the first 5 months of the year (January–May), meteorology plays an important role in enhancing or inhibiting Highveld surface ozone through its sensitivity to ENSO, where cloud cover is likely to be the single most important parameter that inhibits ozone production. More difficult to understand are the statistically significant effects of ENSO on June–September ozone at Verkykkop and Palmer (Figures 11c and 11d). There is evidence that atmospheric transport patterns over southern Africa are influenced by ENSO throughout the lifetime of an episode [*Kanyanga*, 2009] but that study is limited to the El Niño of 1991–1992 and the La Niña of 1999–2000. We believe that October is not sensitive to ENSO at these stations because of the likely dominance of biomass burning at this time of the year. Additionally, ozone and its precursors may be transported into the region from elsewhere in southern Africa by large-scale circulation patterns not affected by ENSO. Overall, for all of the stations except Makalu (Figure 11e), it appears that meteorological effects on ozone are significant in summer and autumn, whereas anthropogenic effects are more pronounced during winter and spring.

A summary of ozone trends over the Highveld as calculated with the regression model appears in Table 6 and Figure 11. Based on annual data, it is seen that no site has a statistically significant trend but some seasonal trends appear. Palmer station exhibits a statistically significant seasonal ozone trend in spring. Makalu and Kendal 2 have statistically significant monthly ozone trends. Makalu shows a negative trend in September, and Kendal 2 shows a positive trend in August. Elandsfontein and Verkykkop do not display any significant ozone trends (Figures 11a and 11c). The Kendal 2 positive trend over one month (Figure 11b) is not enough to make any definitive conclusions about the change in ozone at this location. Negative trends at Palmer and Makalu (Figures 11d and 11e) may be partly due to them having smaller data sets. To generalize, there is not much evidence for an increase in surface ozone over the stations examined; on the contrary, Palmer station displays a pronounced ozone decrease.

5. Conclusions

This study identifies El Niño–Southern Oscillation (ENSO) and NO_x effects on surface ozone variability as well as surface ozone trends over the available time periods at the five Eskom air quality monitoring stations Elandsfontein, Kendal 2, Verkykkop, Palmer, and Makalu located in the South African Highveld. We use a generalized regression model to first fit this model to meteorological variables—temperature, relative humidity, cloud cover, and precipitation that are available from the representative weather station Irene. Then the model is applied to surface ozone time series at the mentioned stations to determine seasonal,

trend, ENSO, and NO_x coefficients. Our results show that the aforementioned meteorological variables are mostly sensitive to ENSO during the South African wet season that lasts approximately from October to March, whereas during the April to September dry season, these variables are only partially sensitive to ENSO.

In terms of ozone, the full Elandsfontein data set from 1990 to 2007 does not exhibit ENSO effects, whereas Elandsfontein data from 1991 to 2004 is sensitive to ENSO for November, December, and February through May. NO_x effects are important in spring. Kendal 2 is affected by ENSO from January to May and by NO_x in July, August, September, and October. Verkykkop shows statistically significant ENSO influences in all of the months of the year except October. The same is true for Palmer. Neither Verkykkop nor Palmer is affected by NO_x anomalies. Both stations are removed from the heaviest industrial zone, which may explain the insensitivity to NO_x. The fifth site, Makalu, does not appear to have any response to ENSO but does respond to NO_x in November–January period. This may be in part attributed to its location near more complex emission sources, implying a different photochemical environment from the other sites investigated here. Generally, we observe that surface ozone is sensitive to ENSO during the months when ENSO most strongly affects the Highveld meteorology and to NO_x mainly in October and November during the southern African biomass burning season.

We also examine surface ozone trends at each of the monitoring stations. Palmer and Makalu exhibit statistically significant negative trends in surface ozone over the spring season and the month of September respectively, whereas Kendal 2 has statistically significant positive ozone trend over August. Verkykkop and Elandsfontein show no statistically significant change in surface ozone. Our trend results are not in agreement with the positive trends of near-surface ozone presented in *Clain et al*. [2009] for 1990–2007 (A. Thompson et al., submitted manuscript, 2014). Further research is needed as Johannesburg-Pretoria region is quickly developing and approaching Megacity status (>10 million population).

This study shows statistically significant results of ENSO having an effect on surface ozone over the South African Highveld. It is likely that ENSO alters meteorological variables that directly affect surface ozone formation primarily during summer and autumn, where El Niño acts to amplify ozone and La Niña acts to reduce ozone. We demonstrate that in the wet season the Highveld surface ozone depends significantly on meteorological variability which is partially explained by ENSO, whereas in the dry season ozone seems to be driven mainly by the biomass burning and ozone advection as well as by various anthropogenic activities. Furthermore, because natural meteorological variability is capable of greatly altering surface ozone, it is imperative that in any study of surface ozone trends, large local climate oscillations are considered during the investigation period. The results of this work invite us to think about other places in the world that may experience similar ENSO teleconnections. How has surface ozone in those places responded to ENSO over the past 20 years?

Acknowledgments

We would like to thank two anonymous reviewers for their valuable input that helped to improve our work. We thank Eskom for providing all of the principal research data, and in particular the air quality monitoring team led by Neil Snow and Eric Lynch who managed the monitoring stations, and Willem Landman from CSIR for explaining seasonal effects of ENSO on southern Africa and Gerrie Coetzee from South African Weather Service for the Irene weather data. We also would like to thank Chris Forest and George Young from Pennsylvania State University for fruitful discussions regarding teleconnections and statistical methods. We are grateful for the C4-SAR (Changing Chemistry in a Changing Climate: Human and Natural Impacts over southern Africa) conference that took place near Johannesburg in June of 2011 with a number of valuable talks regarding climate and air pollution of southern Africa. We thank NASA for funding this research as a part of the SHADOZ (Southern Hemisphere Additional Ozonesondes) program, grant NNX09AJ23G. AMT acknowledges support from the J. W. Fulbright Scholars program for an extended visit to North-West University, Potchefstroom, in 2010–2011.

References

Avnery, S., D. L. Mauzerall, J. Liu, and L. W. Horowitz (2011), Global crop yield reductions due to surface ozone exposure: 1. Year 2000 crop production losses and economic damage, *Atmos. Environ.*, *45*(13), 2284–2296.

Aw, J., and M. J. Kleeman (2003), Evaluating the first-order effect of intraannual temperature variability on urban air pollution, *J. Geophys. Res.*, *108*(D12), 4365, doi:10.1029/2002JD002688.

Balashov, N. V., A. M. Thompson, D. E. Kollonige, G. Coetzee, V. Thouret, and F. Posny (2013), Tropospheric ozone increases in the TTL over the southern African region (1990–2007): Insights from sonde and aircraft profiles, Abstract A51F-0101 presented at 2013 Fall Meeting, AGU, San Francisco, Calif., 9–13 Dec.

Bloomfield, P. (2000), *Fourier Analysis of Time Series: An Introduction*, Wiley, New York.

Bloomfield, P., J. A. Royle, L. J. Steinberg, and Q. Yang (1996), Accounting for meteorological effects in measuring urban ozone levels and trends, *Atmos. Environ.*, *30*(17), 3067–3077.

Clain, G., J.-L. Baray, R. Delmas, R. Diab, J. Leclair de Bellevue, P. Keckhut, F. Posny, J. Metzger, and J. Cammas (2009), Tropospheric ozone climatology at two Southern Hemisphere tropical/subtropical sites, (Reunion Island and Irene, South Africa) from ozonesondes, LIDAR, and in situ aircraft measurements, *Atmos. Chem. Phys.*, *9*, 1723–1734.

Collett, K. S., S. J. Piketh, and K. E. Ross (2010), An assessment of the atmospheric nitrogen budget on the South African Highveld, *S. Afr. J. Sci.*, *106*, 35–43.

Combrink, J., R. D. Diab, F. Sokolic, and E. G. Brunke (1995), Relationship between sufrace, free tropopsheric and total column ozone in two constrasting areas in South Africa, *Atmos. Environ.*, *29*(6), 685–691.

Cooper, O. R., R. S. Gao, D. Tarasick, T. Leblanc, and C. Sweeney (2012), Long-term ozone trends at rural ozone monitoring sites across the United States, 1990–2010, *J. Geophys. Res.*, *117*, D22307, doi:10.1029/2012JD018261.

Cox, W. M., and S. H. Chu (1996), Assessment of interannual ozone variation in urban areas from a climatological perspective, *Atmos. Environ.*, *30*(14), 2615–2625.

Diab, R. D., et al. (1996), Vertical ozone distribution over southern Africa and adjacent oceans during SAFARI-92, *J. Geophys. Res.*, *101*(D19), 23,823–23,833, doi:10.1029/96JD01267.

Diab, R. D., A. Raghunandan, A. M. Thompson, and V. Thouret (2003), Classification of tropospheric ozone profiles over Johannesburg based on mozaic aircraft data, *Atmos. Chem. Phys.*, *3*, 713–723.

Diab, R. D., A. M. Thompson, K. Mari, L. Ramsay, and G. J. R. Coetzee (2004), Tropospheric ozone climatology over Irene, South Africa, from 1990 to 1994 and 1998 to 2002, *J. Geophys. Res.*, *109*, D20301, doi:10.1029/2004JD004793.
Doherty, R. M., D. S. Stevenson, C. E. Johnson, W. J. Collins, and M. G. Sanderson (2006), Tropospheric ozone and El Niño–Southern Oscillation: Influence of atmospheric dynamics, biomass burning emissions, and future climate change, *J. Geophys. Res.*, *111*, D19304, doi:10.1029/2005JD006849.
Duenas, C., M. C. Fernandez, S. Canete, J. Carretero, and E. Liger (2002), Assessment of ozone variations and meteorological effects in an urban area in the Mediterranean Coast, *Sci. Total Environ.*, *299*(1–3), 97–113.
Efron, B., and R. Tibshirani (1993), *An Introduction to the Bootstrap*, Chapman & Hall, New York.
ESKOM (2000), Environmental report 2000, Management of Impacts: Air Quality, *Rep.*, Sandton, South Africa.
Fishman, J., V. G. Brackett, E. V. Browell, and W. B. Grant (1996), Tropospheric ozone derived from TOMS/SBUV measurements during TRACE A, *J. Geophys. Res.*, *101*(D19), 24,069–24,082.
Flynn, J., et al. (2010), Impact of clouds and aerosols on ozone production in Southeast Texas, *Atmos. Environ.*, *44*(33), 4126–4133.
Freedman, D. A. (1981), Bootstrapping regression models, *Ann. Stat.*, *9*(6), 1218–1228.
Goddard, L., and N. E. Graham (1999), Importance of the Indian Ocean for simulating rainfall anomalies over eastern and southern Africa, *J. Geophys. Res.*, *104*(D16), 19,099–19,116.
Higgins, J. J. (2003), *An Introduction to Modern Nonparametric Statistics*, Brooks/Cole, Pacific Grove, Calif.
Jenkin, M. E., and K. C. Clemitshaw (2000), Ozone and other secondary photochemical pollutants: Chemical processes governing their formation in the planetary boundary layer, *Atmos. Environ.*, *34*(16), 2499–2527.
Josipovic, M., H. J. Annegarn, M. A. Kneen, J. J. Pienaar, and S. J. Piketh (2010), Concentrations, distributions and critical level exceedance assessment of SO2, NO2 and O3 in South Africa, *Environ. Monit. Assess.*, *171*(1), 181–196.
Kalnay, E., et al. (1996), The NCEP/NCAR 40-year reanalysis project, *Bull. Am. Meteorol. Soc.*, *77*(3), 437–471.
Kanyanga, J. K. (2009), El Niño Southern Oscillation (ENSO) and atmospheric transport over Southern Africa, PhD thesis, 153 pp., Univ. of Johannesburg, Johannesburg.
Klonecki, A., and H. Levy (1997), Tropospheric chemical ozone tendencies in CO-CH4-NOy-H2O system: Their sensitivity to variations in environmental parameters and their application to a global chemistry transport model study, *J. Geophys. Res.*, *102*(D17), 21,221–21,237.
Laakso, L., et al. (2008), Basic characteristics of atmospheric particles, trace gases and meteorology in a relatively clean Southern African Savannah environment, *Atmos. Chem. Phys.*, *8*(16), 4823–4839.
Laakso, L., et al. (2012), South African EUCAARI measurements: Seasonal variation of trace gases and aerosol optical properties, *Atmos. Chem. Phys.*, *12*(4), 1847–1864.
Landman, W. A., D. DeWitt, D. E. Lee, A. Beraki, and D. Lotter (2012), Seasonal rainfall prediction skill over South Africa: One- versus two-tiered forecasting systems, *Weather Forecasting*, *27*(2), 489–501.
Lelieveld, J., and P. J. Crutzen (1990), Influences of clouds photochemical processes on tropospheric ozone, *Nature*, *343*(6255), 227–233.
Lindesay, J. A. (1988), South-african rainfall, the sourthern oscillation and a southern-hemisphere semi-annual cycle, *J. Climatol.*, *8*(1), 17–30.
Liousse, C., A. Konaré, M. Kanakidou, and K. Pienaar (2012), Africa, in *WMO/IGAC Impacts Of Megacities on Air Pollution and Climate*, edited by T. Zhu et al., pp. 28–58, World Meteorological Organization (WMO), Geneva.
Lourens, A. S., J. P. Beukes, P. G. van Zyl, G. D. Fourie, J. W. Burger, J. J. Pienaar, C. E. Read, and J. H. Jordaan (2011), Spatial and temporal assessment of gaseous pollutants in the Highveld of South Africa, *S. Afr. J. Sci.*, *107*(1–2), 55–62.
Marufu, L., F. Dentener, J. Lelieveld, M. O. Andreae, and G. Helas (2000), Photochemistry of the African troposphere: Influence of biomass-burning emissions, *J. Geophys. Res.*, *105*(D11), 14,513–14,530.
Matooane, M., J. John, R. Oosthuizen, and M. Binedell (2004), Vulnerability of South African communities to air pollution, paper presented at the 8th World Congress on Environmental Health, Durban, South Africa.
Mokgathle, B. B. (2006), Seasonal and diurnal variations of surface ozone on the Mpumalanga Highveld, Masters thesis, 160 pp., North-West Univ., Potchefstroom.
Murazaki, K., and P. Hess (2006), How does climate change contribute to surface ozone change over the United States?, *J. Geophys. Res.*, *111*, D05301, doi:10.1029/2005JD005873.
Norman, R., B. Barnes, A. Mathee, D. Bradshaw, and South African Comparative Risk Assessment Collaborating Group (2007), Estimating the burden of disease attributable to indoor air pollution from household use of solid fuels in South Africa in 2000, *S. Afr. Med. J.*, *97*(8), 764–771.
Randel, W. J., and J. B. Cobb (1994), Coherent variations of monthly mean total ozone and lower stratospheric temperature, *J. Geophys. Res.*, *99*(D3), 5433–5447.
Reason, C. J. C., and D. Jagadheesha (2005), Relationships between South Atlantic SST variability and atmospheric circulation over the South African region during austral winter, *J. Clim.*, *18*(16), 3339–3355.
Rorich, R. P., and J. S. Galpin (1998), Air quality in the Mpumalanga Highveld region, South Africa, *S. Afr. J. Sci.*, *94*(3), 109–114.
Seinfeld, J. H., and S. N. Pandis (2006), *Atmospheric Chemistry and Physics: From Air Pollution to Climate Change*, John Wiley, Hoboken, N. J.
Sillman, S. (1999), The relation between ozone, NOx and hydrocarbons in urban and polluted rural environments, *Atmos. Environ.*, *33*(12), 1821–1845.
Sillman, S., and F. J. Samson (1995), Impact of temperature on oxidant photochemistry in urban, polluted rural and remote environments, *J. Geophys. Res.*, *100*(D6), 11,497–11,508.
Statistics South Africa (2012), Census 2011 Statistical release, *Rep.*, 78 pp., Pretoria.
Stevens, C. S. (1987), Ozone formation in the greater Johannesburg region, *Atmos. Environ.*, *21*(3), 523–530.
Stolarski, R. S., P. Bloomfield, R. D. McPeters, and J. R. Herman (1991), Total Ozone trends deduced from Nimbus 7 Toms data, *Geophys. Res. Lett.*, *18*(6), 1015–1018.
Thomas, R., and Y. Scorgie (2006), Air quality impact assessment for the proposed new coal-fired power station (Kendal North) in the Witbank area, *Rep.*, Airshed Planning Professionals (Pty) Ltd.
Thompson, A. M. (1984), The effect of clouds on photolysis rates and ozone formation in the unpolluted troposphere, *J. Geophys. Res.*, *89*(D1), 1341–1349.
Thompson, A. M. (1992), The oxidizing capacity of the Earth's atmosphere—Probable past and future changes, *Science*, *256*(5060), 1157–1165.
Thompson, A. M., et al. (1996), Ozone over southern Africa during SAFARI-92 TRACE A, *J. Geophys. Res.*, *101*(D19), 23,793–23,807.
Thompson, A. M., J. C. Witte, R. D. Hudson, H. Guo, J. R. Herman, and M. Fujiwara (2001), Tropical tropospheric ozone and biomass burning, *Science*, *291*(5511), 2128–2132.
Trenberth, K. E. (1997), The definition of El Niño, *Bull. Am. Meteorol. Soc.*, *78*(12), 2771.
Tu, J., Z. G. Xia, H. S. Wang, and W. Q. Li (2007), Temporal variations in surface ozone and its precursors and meteorological effects at an urban site in China, *Atmos. Res.*, *85*(3–4), 310–337.

Tyson, P. D. (1986), *Climatic Change and Variability in Southern Africa*, Oxford Univ. Press, Cape Town.
Tyson, P. D., and R. A. Preston-Whyte (2000), *The Weather and Climate of Southern Africa*, Oxford Univ. Press, Cape Town, New York.
Tyson, P. D., F. J. Kruger, and C. Louw (1988), *Atmospheric Pollution and Its Implications in the Eastern Transvaal Highveld*, National Scientific Programmes Unit: CSIR, Pretoria.
Uysal, N., and R. M. Schapira (2003), Effects of ozone on lung function and lung diseases, *Curr. Opin. Pulmonary Med.*, *9*(2), 144–150.
Wilks, D. S. (1997), Resampling hypothesis tests for autocorrelated fields, *J. Clim.*, *10*(1), 65–82.
Wilks, D. S. (2011), *Statistical Methods in the Atmospheric Sciences*, Academic Press, Oxford; Waltham, MA.
Xie, P. P., and P. A. Arkin (1996), Analyses of global monthly precipitation using gauge observations, satellite estimates, and numerical model predictions, *J. Clim.*, *9*(4), 840–858.
Ziemke, J. R., S. Chandra, R. D. McPeters, and P. A. Newman (1997), Dynamical proxies of column ozone with applications to global trend models, *J. Geophys. Res.*, *102*(D5), 6117–6129.
Zunckel, M., K. Venjonoka, J. J. Pienaar, E. D. Brunke, O. Pretorius, A. Koosialee, A. Raghunandan, and A. M. van Tienhoven (2004), Surface ozone over southern Africa: Synthesis of monitoring results during the Cross border Air Pollution Impact Assessment project, *Atmos. Environ.*, *38*(36), 6139–6147.